OPEN

Citation: Cell Death and Disease (2013) 4, e665; doi:10.1038/cddis.2013.154

www.nature.com/cddis

Sorafenib ameliorates bleomycin-induced pulmonary fibrosis: potential roles in the inhibition of epithelial–mesenchymal transition and fibroblast activation

Y-L Chen*[,1,4], X Zhang[2,4], J Bai[1], L Gai[2], X-L Ye[3], L Zhang[2], Q Xu[1], Y-X Zhang[2], L Xu[1], H-P Li*[,2] and X Ding*[,1]

Idiopathic pulmonary fibrosis (IPF) is a serious progressive and irreversible lung disease with unknown etiology and few treatment options. This disease was once thought to be a chronic inflammatory-driven process, but it is increasingly recognized that the epithelial–mesenchymal transition (EMT) contributes to the cellular origin of fibroblast accumulation in response to injury. During the pathogenesis of pulmonary fibrotic diseases, transforming growth factor-β (TGF-β) signaling is considered a pivotal inducer of EMT and fibroblast activation, and a number of therapeutic interventions that interfere with TGF-β signaling have been developed to reverse established fibrosis. However, efficient and well-tolerated antifibrotic agents are not currently available. Previously, we reported the identification of sorafenib to antagonize TGF-β signaling in mouse hepatocytes *in vitro*. In this manuscript, we continued to evaluate the antifibrotic effects of sorafenib on bleomycin (BLM)-induced pulmonary fibrosis in mice. We further demonstrated that sorafenib not only profoundly inhibited TGF-β1-induced EMT in alveolar epithelial cells, but also simultaneously reduced the proliferation and collagen synthesis in fibroblasts. Additionally, we presented *in vivo* evidence that sorafenib inhibited the symptoms of BLM-mediated EMT and fibroblast activation in mice, warranting the therapeutic potential of this drug for patients with IPF.
Cell Death and Disease (2013) **4,** e665; doi:10.1038/cddis.2013.154; published online 13 June 2013
Subject Category: Experimental Medicine

As the most common type of interstitial lung disease, idiopathic pulmonary fibrosis (IPF) is a progressive and generally fatal disorder of unknown etiology that predominantly occurs in middle-aged and elderly adults.[1,2] Although the widely accepted clinical presentation of IPF consists of varying degrees of interstitial fibrosis and parenchymal inflammation, additional diagnostically relevant findings remain largely elusive. IPF is characterized by the loss of respiratory function with marked distortion of lung architecture. The histopathological hallmarks of patients with IPF are known as fibroblast foci, which consist of aggregates of activated fibroblasts that produce excessive levels of extracellular matrix (ECM) within the alveolar space at the site of epithelial cell loss.[2–4] Traditionally, this disease was thought to be a chronic inflammatory-driven response caused by the abnormal accumulation of inflammatory cells such as alveolar macrophages and neutrophils. However, this view has recently been questioned and a growing body of evidence indicates that the progressive fibrotic reaction in IPF was associated with an epithelial-dependent fibroblast-activated process, termed epithelial–mesenchymal transition (EMT).[5–8] Actually, numerous studies elucidate that abnormally activated bronchiolar and alveolar epithelial cells (AECs) express most of cytokines responsible for driving EMT and fibroblast activation. Among these mediators, transforming growth factor-β (TGF-β) is a vital switch.[9,10]

The TGF-β superfamily encompasses a large group of pleiotropic cytokines that regulate a wide array of biological functions ranging from embryonic development to wound repair primarily through a canonical Smad-dependent mechanism.[11,12] TGF-β protein was first described as a master inducer of EMT in normal mammary epithelial cells and was further shown to initiate and maintain EMT in the organ fibrogenesis and tumor metastasis.[13,14] In the lung, repeated acute injuries provoke the cell death of AECs and subsequently increase the proliferative and migratory

[1]State Key Laboratory of Cell Biology, Institute of Biochemistry and Cell Biology, Shanghai Institutes for Biological Sciences, Chinese Academy of Sciences, Shanghai, PRC; [2]Shanghai Pulmonary Hospital, Tongji University School of Medicine, Shanghai, PRC and [3]Ningbo Institute of Medical Sciences, Ningbo University, Zhejiang, PRC
*Corresponding author: Y-L Chen, State Key Laboratory of Cell Biology, Institute of Biochemistry and Cell Biology, Shanghai Institutes for Biological Sciences, Chinese Academy of Sciences, 320 Yueyang Road, Shanghai 200031, PRC. Tel: +86 21 54921412; Fax: +86 21 54921439; E-mail: chenyl@sibcb.ac.cn
or H-P Li, Shanghai Pulmonary Hospital, Tongji University School of Medicine, 507 Zheng Min Road, Shanghai 200433, PRC. Tel: +86 21 65115006; Fax: +86 21 65111298; E-mail: liw2013@126.com
or X Ding, State Key Laboratory of Cell Biology, Institute of Biochemistry and Cell Biology, Shanghai Institutes for Biological Sciences, Chinese Academy of Sciences, Room 741, Biochemistry Building, 320 Yueyang Road, Shanghai 200031, PRC. Tel: +86 21 54921411; Fax: +86 21 54921439; E-mail: xyding@sunm.shcnc.ac.cn
[4]These authors contributed equally to this work.
Keywords: sorafenib; TGF-β signaling; pulmonary fibrosis; EMT; fibroblast activation
Abbreviations: AEC, alveolar epithelial cell; α-SMA, α-smooth muscle actin; BLM, bleomycin; DMEM, Dulbecco's modified Eagle's medium; ECM, extracellular matrix; EdU, 5-ethynyl-2′-deoxyuridine; EMT, epithelial–mesenchymal transition; FSP1, fibroblast-specific protein-1; Hyp, hydroxyproline; IPF, idiopathic pulmonary fibrosis; MMP, matrix metalloproteinase; MTT, 3-(4,5-dimethylthiazol-2-yl)-2,5-diphenyltetrazolium bromide; TGF-β, transforming growth factor-β; TIMP, tissue inhibitors of metalloproteinase; TKI, tyrosine-kinase inhibitor
Received 01.1.13; revised 01.4.13; accepted 03.4.13; Edited by G Melino

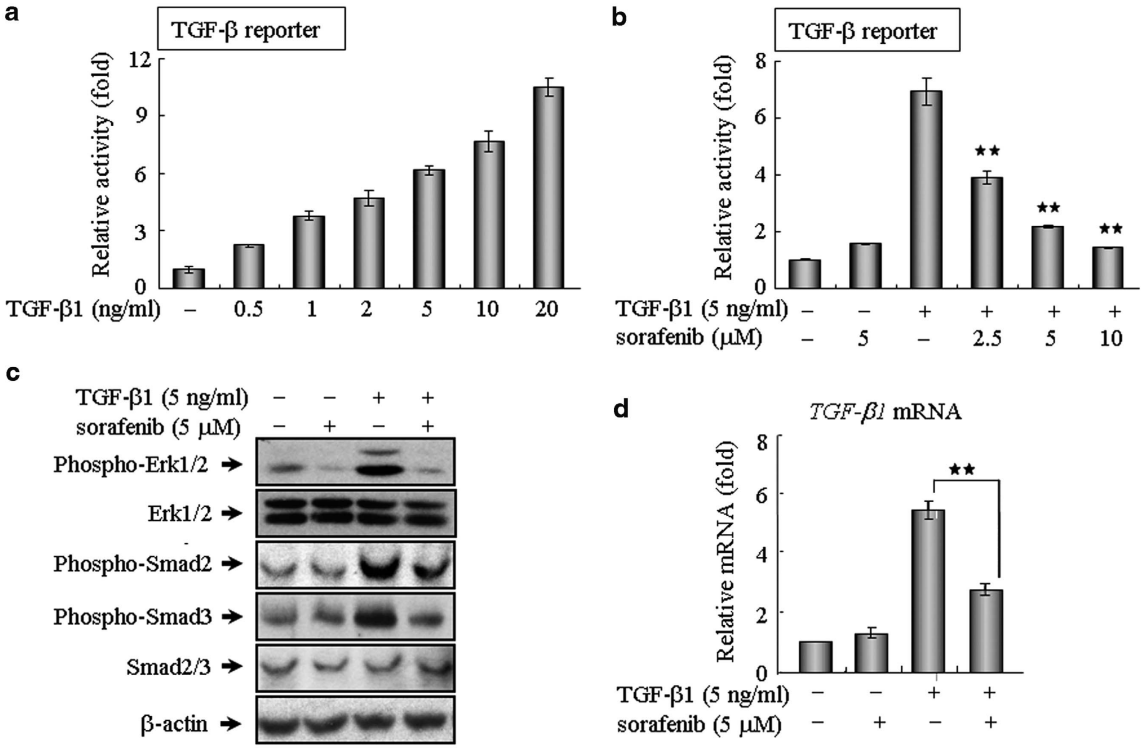

Figure 1 Sorafenib blocks TGF-β signaling *in vitro*. (**a** and **b**) Sorafenib antagonizes TGF-β-induced reporter activity in a dose-dependent manner. As described in Materials and Methods, NIH 3T3 cells seeded in 24-well plates were transfected with 200 ng of the $(CAGA)_{12}$-Lux reporter, incubated with TGF-β1 and/or sorafenib, and then analyzed using a luciferase assay. (**c**) NIH 3T3 fibroblasts were treated as indicated for 3 h and assayed by western blot analysis to assess the phosphorylation of Smad2, Smad3 and ERK1/2. β-Actin was used as a loading control. (**d**) After treatment as indicated for 24 h, A549 cells were subjected to real-time qPCR analysis. All of the assays were performed in triplicate, and the data are shown as the mean values ± S.E. The asterisks denote significant differences ($P<0.01$) within experiments, as determined by the Student's *t*-test

capacity of AECs in a frustrated effort of lung repair. Abnormally activated AECs secrete latent TGF-β1 to promote alveolar EMT in AECs and transdifferentiation of quiescent fibroblasts into myofibroblasts, which contribute to the excessive production of fibrillar collagens.[2,15] Indeed, the biologically active form of TGF-β1 was shown to be aberrantly expressed in epithelial cells that line the honeycomb cysts in the lungs of patients suffering from IPF.[16,17] Therefore, given the established actions of TGF-β on EMT and collagen synthesis, strategies that utilize proteins or small chemicals to disrupt TGF-β production and/or block the associated signal transduction have important theoretical and therapeutic potential in the clinical treatment of pulmonary fibrosis.

Heretofore, the treatment for lung diseases like IPF has focused largely on the amelioration of potential inciting processes, such as inflammation. However, the long-term survival of IPF patients remains poor, and the anti-inflammatory therapy for IPF with oral glucocorticoids is often ineffective.[2–4] Till now, no substantial therapeutic interventions have been developed to reverse established fibrosis or even halt the chronic progression to respiratory failure. Previously, we reported the identification of sorafenib, an oral multikinase inhibitor that antagonized TGF-β1-mediated EMT and apoptosis in mouse hepatocytes.[18] In the present study, we demonstrated that sorafenib counteracted the profibrotic activity of TGF-β signaling and thereby improved bleomycin (BLM)-mediated pulmonary fibrosis in mice. We further demonstrated that sorafenib suppressed TGF-β1-induced EMT in A549 cells and primary cultured AECs. Meanwhile, sorafenib reduced the proliferation and ECM production in fibroblasts. In addition, we provided *in vivo* evidence that sorafenib inhibited apparent EMT and fibroblast activation in the murine pathogenesis of pulmonary fibrosis induced by BLM, suggesting a potential therapeutic option in the treatment of IPF.

Results

Sorafenib antagonizes TGF-β-mediated Smad and non-Smad signaling. As a star molecule in cancer therapy, sorafenib is the first oral multi-kinase inhibitor approved by the Food and Drug Administration for the clinical treatment of a variety of tumor types.[19,20] Prior studies have largely focused on the ability of sorafenib to potently inhibit angiogenesis and tumor growth by blocking a number of receptor tyrosine kinases and Raf kinases.[19–21] However, aside from the established clinical benefits of sorafenib, this drug likely has a much broader function than is currently known. Here, we evaluated the impact of sorafenib on TGF-β signaling in NIH 3T3 cells using a $(CAGA)_{12}$-Lux reporter, which contains 12 copies of the Smad-binding site. Notably, this reporter was capable of being activated in response to a wide range of TGF-β1 concentrations and was inhibited in a dose-dependent manner by sorafenib (Figures 1a and b). This finding was validated in different cell lines, including human kidney 293T cells, human A549 cells and mouse

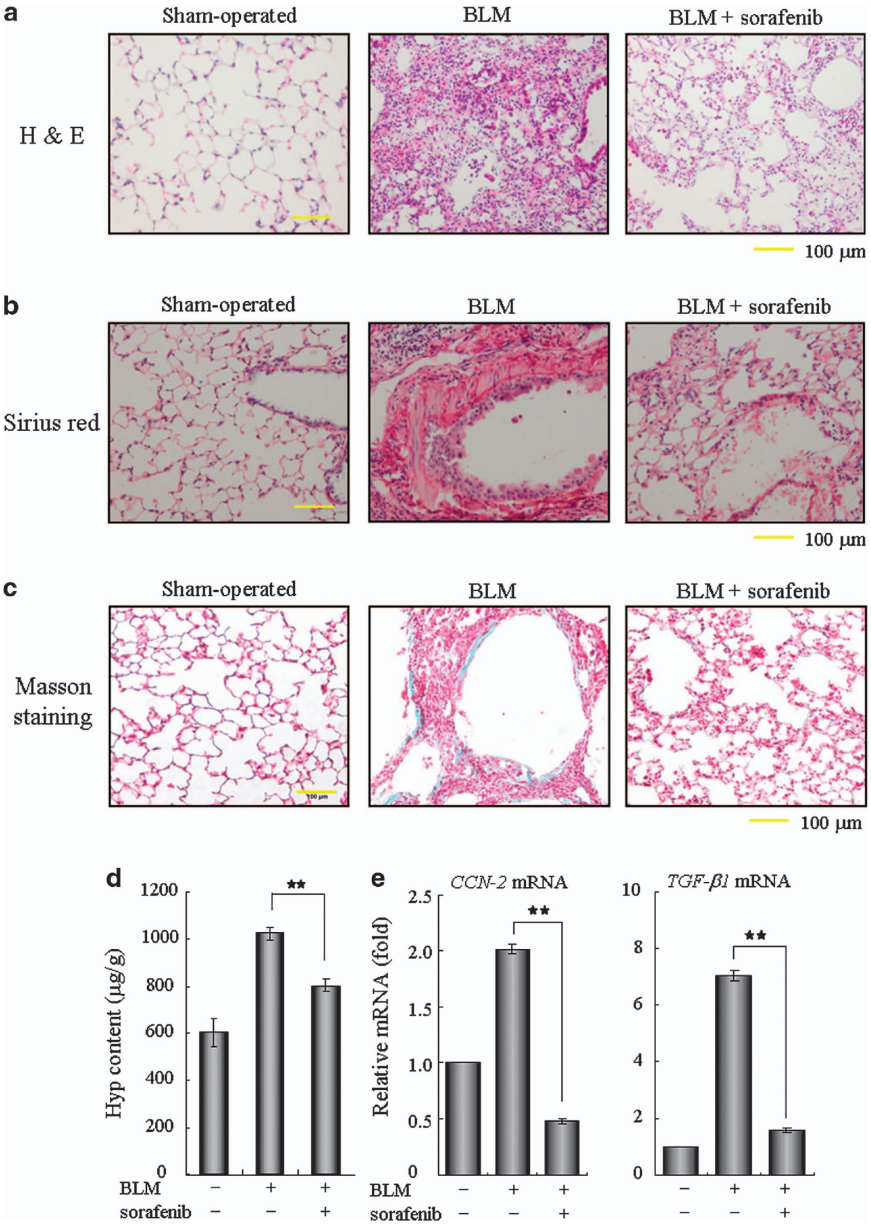

Figure 2 Sorafenib ameliorates bleomycin (BLM)-induced pulmonary fibrosis *in vivo*. Mice were treated with 3.5 mg/kg BLM once at day 0 and subsequently received sorafenib (5 mg/kg) or vehicle by gavage once per day for 12 days (from days 3 to 14). (**a**) Pulmonary tissue sections were prepared at day 14 and stained with hematoxylin and eosin (H&E) for routine examination. (**b** and **c**) The sections were also subjected to Sirius red or Masson's trichrome staining for the visualization of collagen deposition. (**d**) The hydroxyproline (Hyp) content of the pulmonary tissues ($n = 5$ for each group) was measured at day 28 and is presented as micrograms of Hyp per gram of wet weight (μg/g). (**e**) Real-time PCR was performed to detect the expression of *CCN-2* and *TGF-β1* in the pulmonary tissues from each group. $^{**}P < 0.01$; as determined using Student's *t*-test

AML12 hepatocytes (Supplementary Figure 1), revealing that sorafenib antagonized TGF-β signaling *in vitro* regardless of the cell type. To further explore the intracellular signal transduction mechanism, we first examined the effects of sorafenib on the canonical Smad-dependent pathway, which requires a family of signal transducers called R-Smads (Smad2 and Smad3). As shown in Figure 1c, sorafenib could evidently abrogate TGF-β-mediated phosphorylation of Smad2 and Smad3 at a workable concentration of 5 μM. Because TGF-β also elicits signal responses through the activation of MAP kinase signaling,[11,12] we then investigated whether sorafenib negatively regulated this kinase cascade and found sorafenib suppressed the phosphorylation of p44/42 MAPK (Erk1/2) in mouse fibroblasts, indicating that sorafenib effectively blocked TGF-β signaling via the inhibition of both Smad and non-Smad pathway. In addition, we examined whether sorafenib impaired the endogenous level of *TGF-β1* transcripts, which are known to be expressed in an autocrine manner.[11] Indeed, the application of sorafenib markedly reduced the expression and production of *TGF-β1* transcripts (Figure 1d).

Sorafenib improves BLM-induced pulmonary fibrosis in mice. Numerous studies have recognized TGF-β as a

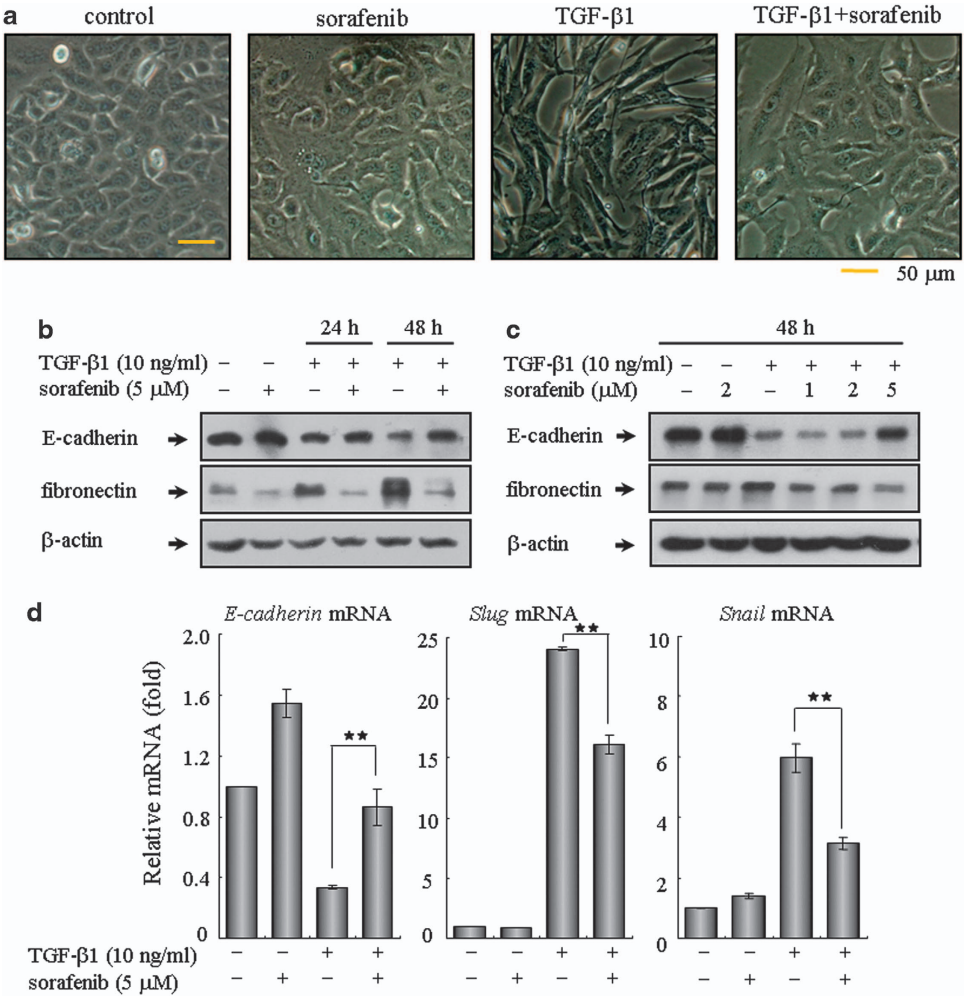

Figure 3 Treatment with sorafenib inhibits TGF-β1-induced EMT in alveolar epithelial A549 cells. A549 cells were treated with TGF-β1 (10 ng/ml) and sorafenib (5 μM) for 24 or 48 h. The cells treated with vehicle (DMSO) only served as controls. The extent of EMT was determined by assessing the (**a**) morphological changes and (**b**) protein expression profiles of E-cadherin and fibronectin. Similarly, cells were incubated with TGF-β1 (10 ng/ml) and increasing concentrations of sorafenib (1, 2 and 5 μM) for 48 h. The inhibitory effect of sorafenib on EMT was further examined by (**c**) immunoblot analysis and (**d**) real-time qPCR on related transcriptional factors, including *E-cadherin*, *Slug* and *Snail*. $^{**}P<0.01$; as determined using Student's *t*-test

profibrogenic master cytokine;[8–10] therefore, we speculated that sorafenib may have therapeutic potential for pulmonary fibrosis *in vivo* by disrupting TGF-β signaling. To test this hypothesis, we established an experimental acute lung injury model induced by BLM. Using this animal model, we found that treatment with sorafenib by daily gavage at a dose of 5 mg/kg body weight was well tolerated, as no drug-related adverse events were observed. As determined by hematoxylin and eosin staining of lung sections, the intratracheal injection of BLM led to the destruction of normal pulmonary architecture, the prominent proliferation of fibroblasts, the infiltration of inflammatory cells and the extensive deposition of fibrillar collagen. Impressively, we observed remarkable improvement in these pathological changes after the administration of sorafenib (Figure 2a). Likewise, the deposition of collagen fibers was largely reduced after the administration of sorafenib, as illustrated by the Sirius red- and Masson's trichrome-positive areas (Figures 2b and c). We then measured the pulmonary hydroxyproline (Hyp) contents of five mice from each group to quantify the extent of pulmonary fibrosis, as Hyp is a major constituent of collagen. Compared with the BLM group, the Hyp level was reduced by approximately 22% after treatment with sorafenib (Figure 2d), suggesting a protective role of sorafenib in counteracting ECM accumulation. In addition, the expression levels of the potent pro-fibrotic factors *TGF-β1* and *CCN2* (connective tissue growth factor) were reduced around 75% in the sorafenib-treated group (Figure 2e). Taken together, these results reveal an antifibrotic effect of sorafenib that protects against pulmonary fibrosis *in vivo*.

Sorafenib counteracts TGF-β1-induced EMT in A549 cells and primary AECs. The above findings prompted us to further explore the detailed mechanism underlying the antifibrotic effects of sorafenib. During the pathogenesis of pulmonary fibrotic diseases, the main effector cells responsible for the excessive ECM production are activated fibroblasts, which arise from alveolar EMT of AECs and proliferation of resident fibroblasts.[15] Hence, evaluation of the effects of sorafenib on the derivation of lung fibroblasts

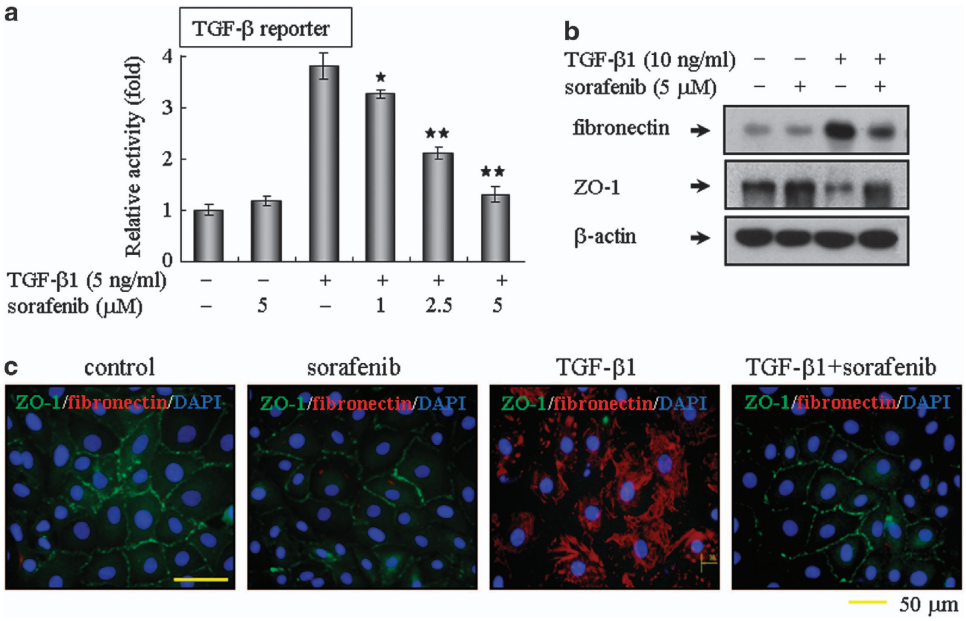

Figure 4 Sorafenib counteracts TGF-β1-induced EMT in primary cultured alveolar epithelial type II cells. (**a**) Sorafenib blocks TGF-β-mediated reporter activity. Primary cultured alveolar epithelial type II cells were transfected with the $(CAGA)_{12}$-Lux reporter, cultured with TGF-β1 and sorafenib as indicated, and analyzed using a luciferase assay. (**b**) In addition, primary cultured alveolar epithelial type II cells were incubated with TGF-β1 (10 ng/ml) in the absence or presence of sorafenib (5 μM) for 48 h. The extent of EMT was then evaluated by immunoblot analysis. (**b**) EMT was also examined by immunofluorescent staining for the epithelial marker ZO-1 (red) and the mesenchymal marker fibronectin (green). The nuclei were labeled with DAPI. The bar represents 50 μm for each section. $^*P<0.05$; $^{**}P<0.01$; as determined using Student's *t*-test

seems timely and pertinent. First, we assess the impact of sorafenib on EMT using human A549 cells, an alveolar type II epithelial cell line that has been widely used as an ideal *in vitro* model to study EMT, carcinogenesis and drug metabolism.[22] Forty-eight hours of exposure to TGF-β1 caused A549 cells to undergo EMT, during which the cells lost their epithelial honeycomb-like morphology and obtained a spindle-like shape (Figure 3a). Aside from these morphological changes, the expression of the adherens junction protein E-cadherin was decreased and the expression of the intermediate filament protein fibronectin was upregulated (Figure 3b). As expected, treating A549 cells with sorafenib reversed the TGF-β1-induced EMT, as shown by phenotypic cellular alterations (Figure 3a) and the expression profiles of EMT markers (Figure 3b). We also treated cells with increasing doses of sorafenib after TGF-β1 stimulation. As shown in Figure 3c, sorafenib mediated cellular resistance to EMT in a dose-dependent manner. Because Snail and Slug are zinc-finger transcriptional repressors that have been identified as the immediate-early response genes for TGF-β during EMT,[23] we then examined whether sorafenib regulates these EMT-related transcription factors. As shown in Figure 3d, the mRNA levels of *Snail* and *Slug* were markedly induced following treatment with TGF-β1 and were remarkably decreased after treatment with sorafenib. Furthermore, although TGF-β1 elevated the migration of A549 cells, this process was also repressed by sorafenib (Supplementary Figure 2).

Next, we confirmed the roles of sorafenib on TGF-β1-induced EMT in primary rat AECs. Consistent with the results observed in A549 cells, sorafenib could also blunt the TGF-β1-dependent reporter activity in primary cultured type II AECs (Figure 4a). Moreover, sorafenib abrogated the reduction in the expression of tight junction protein ZO-1 and the increase in fibronectin expression (Figure 4b). Meanwhile, co-staining for ZO-1 and fibronectin revealed that sorafenib reversed the TGF-β1-induced EMT in primary cultured type II AECs (Figure 4c). Collectively, these data provide *in vitro* evidence that sorafenib maintains the epithelial properties of AECs and prevents AECs from transitioning to a mesenchymal-like phenotype in response to TGF-β1.

Sorafenib inhibits cell proliferation and induces progressive apoptosis in mouse fibroblasts. Because (myo)fibroblasts undergo autonomous proliferation and produce excessive matrix proteins, which resemble a wound-healing process during pulmonary fibrosis,[2,4,24] we subsequently investigated the ability of sorafenib on the modulation of fibroblast proliferation and activation in NIH 3T3 cells. As determined by 3-(4,5-dimethylthiazol-2-yl)-2,5-diphenyltetrazolium bromide (MTT) assay, TGF-β1 stimulation resulted in an increased number of viable fibroblasts, whereas the cell viability was evidently reduced by sorafenib in a dose- and time-dependent manner (Figure 5a). This finding prompted us to explore the impact of this compound on cell growth using 5-ethynyl-2′-deoxyuridine (EdU) incorporation assay. As shown in Figure 5b, the DNA synthesis was rapidly decreased in the cells following treatment with sorafenib. In addition, FACS analysis showed that exposure of fibroblasts to sorafenib eventually led to an accumulation of cells in the G0/G1 phase and sub-G1 population (Figures 5c and d), suggesting that sorafenib exerts its antiproliferative activity by inducing cell cycle arrest and apoptosis. Further experiments revealed that sorafenib elicited an

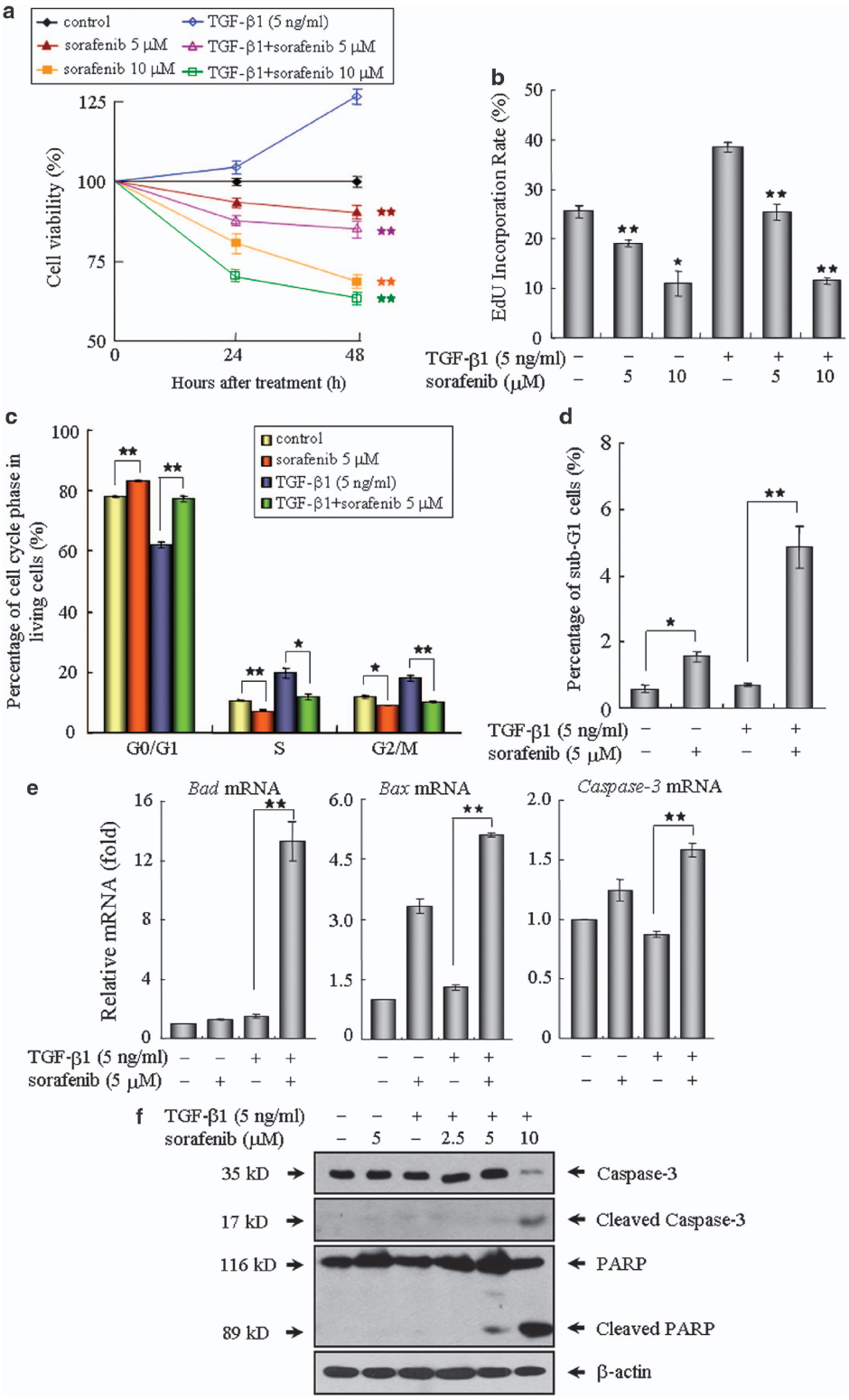

Figure 5 Sorafenib inhibits cell proliferation and promotes apoptosis in mouse NIH 3T3 fibroblasts. (**a**) The cell viabilities of NIH3T3 fibroblasts treated as indicated were measured by MTT assay at 24 and 48 h, respectively. (**b**) After treatment with TGF-β1 and/or sorafenib for 48 h, the fibroblasts were incubated with EdU (25 μM) in medium for an additional 3 h. The ratio of EdU-positive cells to Hoechst-labeled cells in each group was calculated. (**c**) The effects of sorafenib on the cell cycle profiles were further evaluated by flow cytometry. (**d**) The histogram indicates quantitative assessment of sub-G1 cell populations after propidium iodide staining. The impact of sorafenib on cell apoptosis was further determined by (**e**) real-time qPCR and (**f**) immunoblot analysis on related proapoptotic genes. $^{*}P<0.05$; $^{**}P<0.01$; as evaluated using Student's *t*-test. Abbreviations: M, mitosis; S, DNA duplication phase; G0/G1, gap between end of M-phase and start of S-phase; G2, gap between end of S-phase and start of M-phase

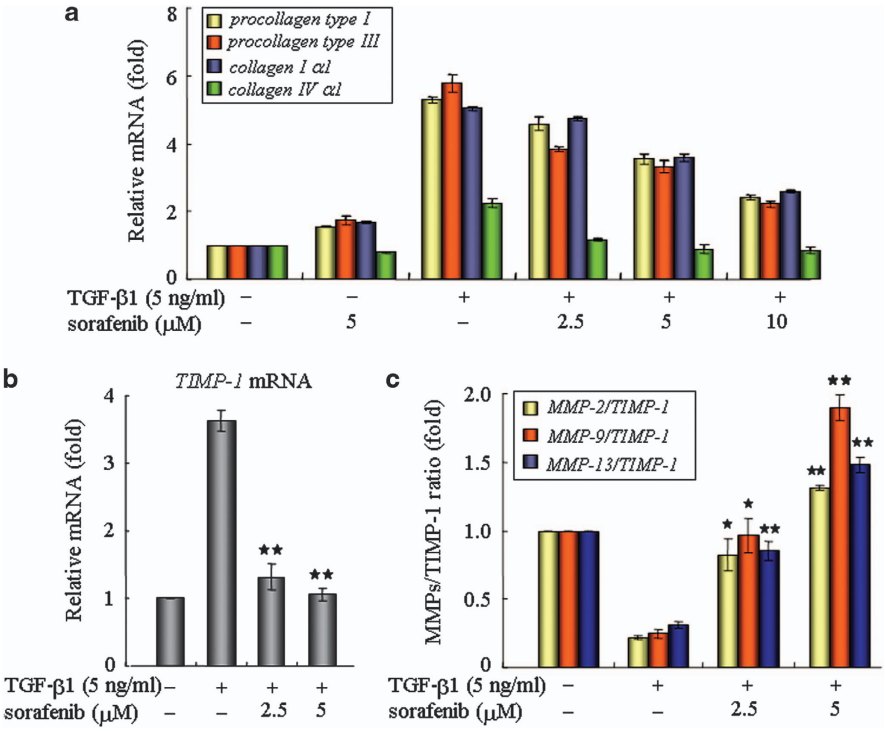

Figure 6 Sorafenib reduces collagen production and ECM accumulation in NIH 3T3 cells. After treatment with TGF-β1 and/or sorafenib for 48 h, mouse NIH3T3 fibroblasts were subjected to real-time qPCR for detecting the effects of sorafenib on the transcriptional levels of (**a**) collagens, (**b**) TIMP-1 and (**c**) MMPs. $^{*}P<0.05$; $^{**}P<0.01$; as determined using Student's *t*-test

increased expression of pro-apoptotic genes including *Bad*, *Bax* and *Caspase 3* (Figure 5e). In line with these real-time qPCR results, treatment with sorafenib also produced the cleaved forms of Caspase-3 and poly (ADP-ribose) polymerase, which are considered reliable markers of apoptosis, and the pro-apoptotic effects of sorafenib became pronounced in the presence of a high concentration of 10 μM (Figure 5f).

Sorafenib reduces collagen production and ECM accumulation in fibroblasts. Afterwards, we examined whether sorafenib treatment could eliminate collagen production in fibroblasts, which are central contributors of ECM deposition in the lung. In response to external TGF-β1 stimulation, fibroblasts upregulated the production of fibrotic matrix components, such as types I, III and IV collagens. Interestingly, these changes were substantially attenuated after treatment with sorafenib (Figure 6a), suggesting an antifibrotic role of sorafenib in counteracting ECM production. These results were further supported by assessing the expression profiles of matrix metalloproteinases (MMPs) and the tissue inhibitors of MMPs (TIMPs), which are essential secretions known to maintain ECM turnover and homeostasis.[22,25] As shown in Figure 6b, the levels of *TIMP-1* mRNA were rapidly induced in response to TGF-β1 and were significantly decreased by treatment with sorafenib. Moreover, sorafenib raised the ratio of MMPs/TIMP-1, leading to a net destruction of ECM in fibroblasts (Figure 6c). Similarly, the antifibrotic effects of sorafenib were confirmed in culture AECs with essentially the same results (Supplementary Figure 3). Therefore, it appears that, sorafenib mediates the inhibition of ECM accumulation in both fibroblasts and AECs.

Sorafenib prevents the EMT phenotype and fibrogenic activation of pulmonary fibroblasts i*n vivo*. The *in vitro* results outlined above encouraged us to further examine the roles of sorafenib on EMT occurrence and fibroblast activation in the mouse lung injury model. Consistent with our histological findings in Figure 2, the loss of lung epithelium and the proliferation of fibroblasts (including those derived through EMT) were observed at day 14 after BLM administration, as characterized by immunohistochemistry of E-cadherin and fibroblast-specific protein-1 (FSP1, also known as S100A4). In sorafenib-treated mice, the loss of E-cadherin expression in the alveolar epithelium was largely reversed and the accumulation of FSP1-positive fibroblasts was dramatically decreased (Figures 7a and b). Likewise, an apparent EMT phenomenon in the intratracheal BLM model was detected by identifying some E-cadherin/FSP1 double-positive cells, which reflect their epithelial origin and a possible intermediate transitional stage of EMT (Figure 7c). Interestingly, this number of epithelial-derived fibroblasts and the expression of FSP1 were both reduced after treatment with sorafenib, suggesting that sorafenib impeded the BLM-induced EMT phenomenon *in vivo*. Next, lung sections were immunostained for α-smooth muscle actin (α-SMA), a reliable marker of activated fibroblasts and myofibroblasts. As shown in Figure 7d, α-SMA was not expressed in interstitium and was restricted to the vessel walls in the saline control mice. Two weeks after administration of BLM, a small portion of myofibroblasts expressing α-SMA in the interstitium were

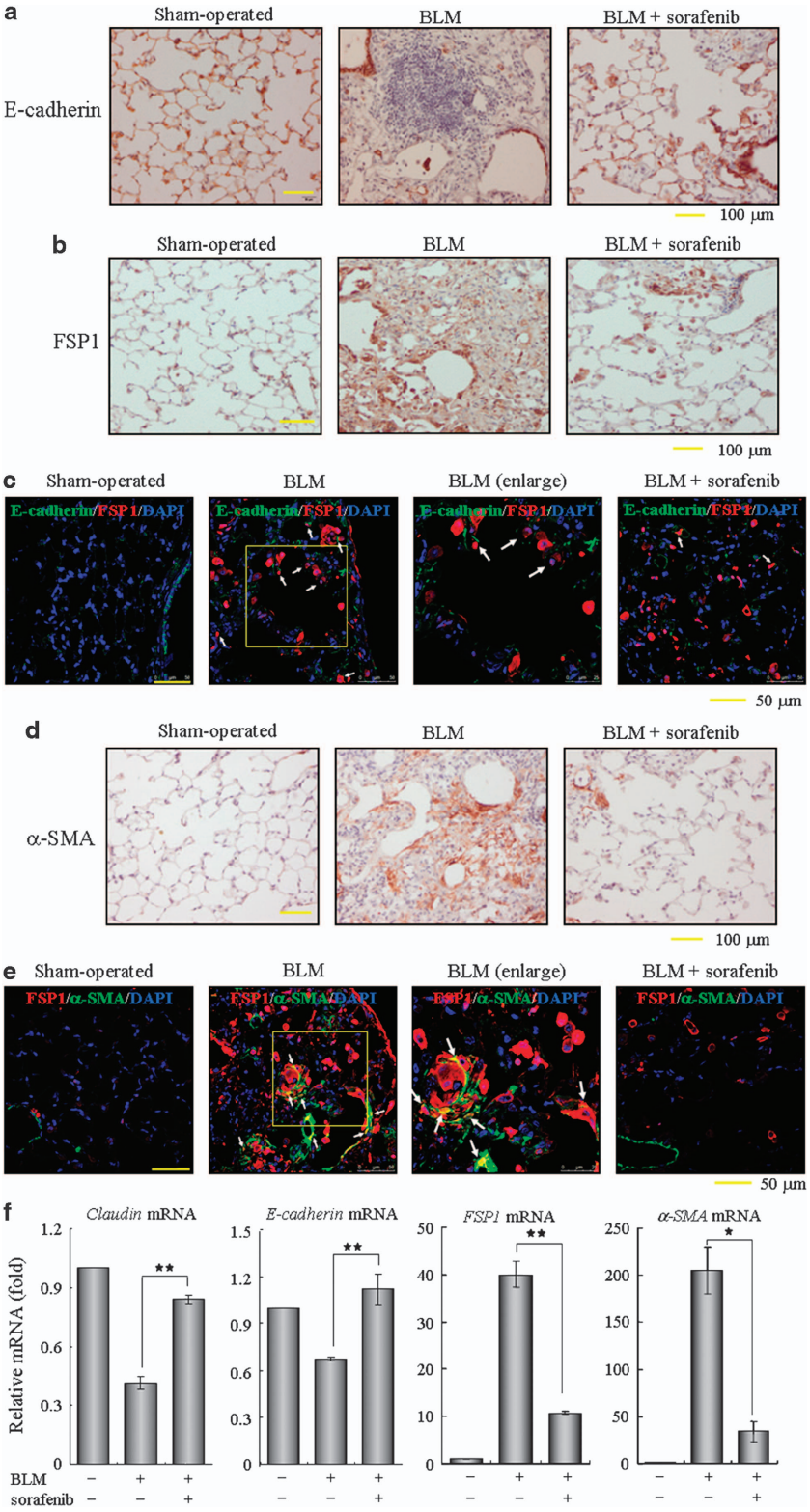

Figure 7 Sorafenib inhibits the EMT phenotype and fibroblast activation *in vivo*. Following a single treatment with 3.5 mg/kg bleomycin (BLM) at day 0, the mice received sorafenib (5 mg/kg) or vehicle by gavage once per day for 12 days (from days 3 to 14). (**a**–**e**) The sections of pulmonary tissues were subjected to immunohistochemical analysis using antibodies as indicated in the figures. Brown coloration indicates positive staining and *white arrows* point to representative double-positive cells. (**f**) Real-time PCR was performed to detect the mRNA levels of *Claudin*, *E-cadherin*, *FSP1* and *α-SMA* in the pulmonary tissues from each group. $^{*}P<0.05$; $^{**}P<0.01$, sorafenib-treated group *versus* BLM-treated group

colocalized with FSP1 (Figure 7e). Expectably, a fewer double-positive cells were found in the lung sections from mice that continuously received sorafenib for 12 days, implicating that sorafenib suppresses the differentiation capacity of lung fibroblasts into myofibroblasts. In addition, we measured the pulmonary expression of these typical markers and confirmed that sorafenib largely relieved the effects of BLM administration on the expression of *Claudin-1*, *E-cadherin, FSP1* and α-*SMA* (Figure 7f). Taken together, these data provide *in vivo* evidence that sorafenib protects against the EMT phenotype and fibroblast activation in murine BLM-induced pulmonary fibrosis.

Discussion

IPF is a complex disease with a poor prognosis and ineffectiveness to currently available therapies, reflecting our limited understanding of the basic mechanisms involved in the pathogenesis of this progressive and fatal disease. To our current knowledge, TGF-β signaling is essential in a number of profibrotic processes including EMT, fibroblast activation, and eventual ECM production and deposition.[1,2] Till now, interventions aimed at eliminating latent TGF-β signaling at various transduction steps have been successfully developed in animal models. For example, the gene transfer of Smad7 or dominant-negative TGF-β receptors was shown to prevent fibrosis in the rodent lung and other organ.[26,27] Aside from these gene therapy approaches, small chemicals targeting this signaling cascade have strong therapeutic potential in clinical settings. In the present study, we first identified a novel property of sorafenib to antagonize TGF-β signaling through reducing the both levels of intracellular signal transduction (Smad-dependent and Smad-independent pathway) and TGF-β1 production (Figures 1c and d), and then extended these *in vitro* findings to an *in vivo* mouse model whereby treatment with sorafenib was proved to be effective in the amelioration of pulmonary fibrosis (Figure 2). Based on these encouraging data generated from cellular and animal models of lung fibrosis in this study, considerable therapeutic benefits of sorafenib could be expected to improve IPF care. Importantly, the use of sorafenib has an exclusive advantage in its safety, efficacy and tolerability has already been well documented, as sorafenib is the Food and Drug Administration-approved oral agent for patients with several types of human malignancies.[19,20] Taking into account the beneficial effects of sorafenib in experimental studies of hepatic cirrhosis and pulmonary hypertension,[28–31] we believe this chemical may have a much broader role in clinical medicine and will be considered more than just an anti-cancer drug.

EMT is a dynamic cellular process that allows polarized, immotile epithelial cells to convert into motile mesenchymal cells.[10] In addition to the essential role that EMT has in tissue remodeling and tumor metastasis, emerging *in vivo* evidence also elucidates EMT as an important source of myofibroblasts in progressive pulmonary, renal and hepatic fibrosis.[5–7,32,33] Here, we observed that sorafenib treatment not only counteracted the TGF-β1-mediated EMT process in both A549 epithelial cells and primary AECs *in vitro* (Figure 3 and Figure 4), but also diminished the occurrence of EMT phenotype in the parenchymal alveolar areas following BLM stimulation *in vivo* (Figure 7c), suggesting that the antifibrotic effects of sorafenib is at least partly due to its interference with the TGF-β1-induced EMT. Because TGF-β can also promote EMT and increase the migratory and invasive properties of tumor cells though Smad proteins during carcinogenesis,[12,34] the inhibition of sorafenib on EMT in A549 lung adenocarcinoma cells (Figure 3 and Supplementary Figure 2) may provide a reasonable explanation for its clinical use in tumor control and reduced cancer metastasis.

IPF is characterized by the proliferation of fibroblasts in fibrotic foci that contain bundles of polymerized collagens. Unlike in physiological wound repair, where fibroblast activation is spontaneously reversible, the fibroblast activation coupled with excessive ECM production is perpetuated during fibrogenesis.[24,35] Considering the central role of activated fibroblasts as in IPF, we also evaluated the impact of sorafenib on the cell cycle and collagen synthesis of fibroblasts. Here, we found that sorafenib could inhibit fibroblast proliferation and induce their apoptosis (Figure 5), which is consistent with previous observations on the activity of sorafenib in various tumor cells.[21,36] Furthermore, sorafenib inhibited the expression of several types of collagens and elevated the ratio of MMPs/TIMP-1 (Figure 6), thereby potentially accelerated the degradation of ECM proteins to reverse established fibrosis. Taken together, this study provides new insights into the possible mechanism in which sorafenib substantially represses TGF-β signaling and subsequently inhibits alveolar EMT, fibroblast activation and ECM production, thus leading to a remarkable improvement in pulmonary fibrosis.

Over the past two decades, the successful development of tyrosine-kinase inhibitors (TKIs) that disrupt several fundamental signaling pathways has marked a notable advance in the fight against cancer.[37] As ongoing clinical research have demonstrated that tyrosine kinases are key mediators of fibrotic, proliferative and inflammatory disorders of the lung and other organs, it is reasonable to expect these TKIs to have a better chance of efficacy for the clinical treatments of other diseases, such as fibrosis. Besides sorafenib, the antifibrotic effectiveness of several TKIs targeting PDGFR and VEGFR has already been observed in different animal models.[38–41] Despite improved insights into this therapeutic avenue, challenges and uncertainties remain in translating preclinical studies to effective drug therapies. Yet imatinib, like sorafenib as a TKI, was originally proved to protect against fibrogenesis in rodent models of lung injury, but failed to benefit patients with IPF in phase II clinical trials.[38,42] Keeping in mind the limitations of translational researches in animal models into clinical practice, we believe that our findings will be promising for consideration of sorafenib as an antifibrotic drug. Certainly, more detailed sets of such investigations will be performed to warrant its potential usefulness in the future applications.

In conclusion, we here demonstrate that sorafenib inhibits the profibrogenic activity of TGF-β signaling and ameliorates BLM-mediated lung fibrosis, suggesting an attractive pharmacological tool for the treatment of IPF and other fibrotic disorders.

Materials and Methods

Reagents and antibodies. Recombinant human TGF-β1 was purchased from R&D Systems (Minneapolis, MN, USA), and sorafenib (Nexavar or BAY

43-9006) was manufactured by Bayer Pharmaceuticals (West Haven, CT, USA). The primary antibodies described in this paper include β-actin (Sigma-Aldrich, St Louis, MO, USA), Caspase-3 (Cell Signalling Technology, Beverly, MA, USA), Cleaved Caspase-3 (Asp175; Cell Signaling Technology), E-cadherin (Cell Signaling Technology; BD Biosciences, San Diego, CA, USA), Erk1/2 (Cell Signaling Technology), Phospho-Erk1/2 (Thr202/Tyr204; Cell Signaling Technology), fibronectin (Sigma-Aldrich), FSP1 (Dako, Glostrup, Denmark), poly (ADP-ribose) polymerase (Cell Signaling Technology), α-SMA (Sigma-Aldrich), Smad2/3 (BD Biosciences), Phospho-Smad2 (Ser465/467; Cell Signaling Technology), Phospho-Smad3 (Ser423/425; Invitrogen, San Francisco, CA, USA) and ZO-1 (Invitrogen).

Animals. Female Sprague–Dawley rats weighing 300–350 g and C57BL/6 mice weighing 23–25 g were purchased from the Shanghai Experimental Animal Center of the Chinese Academy of Sciences, Shanghai, PRC. In compliance with the relevant guidelines, all of the animals received humane care and had free access to food and water during the study. All of the procedures were approved by the Laboratory Animal Care and Use Committees of the Shanghai Institutes for Biological Sciences.

Cell culture and isolation. Human A549 cells were obtained from ATCC (Manassas, VA, USA), and cultured in Dulbecco's modified Eagle's medium (DMEM) supplemented with 10% fetal bovine serum (Biochrom, Berlin, Germany) at 37 °C with 5% CO_2. NIH 3T3 fibroblasts were grown in DMEM containing 10% bovine calf serum.

The type II AECs in primary culture were isolated from the lungs of adult female Sprague–Dawley rats by lavage and perfusion with elastase, according to previously described methods.[43] The freshly isolated AECs were then collected by centrifugation and seeded in DMEM containing 10% fetal bovine serum. The viability of the cells was determined by trypan blue exclusion, and the cell samples with viabilities greater than 95% were used in the subsequent assays.

DNA transfection and luciferase assay. A549 cells were seeded into 24-well plates and transiently transfected with 200 ng of the $(CAGA)_{12}$-Lux reporter, which encodes 12 copies of the canonical CAGA Smad DNA-binding sequence. As an internal control, the cells in each well were co-transfected with 5 ng of the pRL-SV40 plasmid, which expresses *Renilla* luciferase. At 24 h post-transfection, the cells were transferred into serum-free medium supplemented with TGF-β1 (5 ng/ml) and incubated for an additional 12 h before harvesting. The luciferase activity was measured using a Dual Luciferase Reporter Assay System (Promega, Madison, WI, USA) and normalized to the *Renilla* luciferase activity in each sample. All of the assays were performed in triplicate, and the data are shown as the mean values ± S.E. of at least three independent experiments.

Western blotting. To detect the expression levels of epithelial and mesenchymal markers, A549 cells were treated as indicated in the figure legends, lysed in 200 μl of lysis buffer and subjected to western blot analysis.[44] Approximately 50 μg of total protein was separated by SDS-PAGE, transferred to a PVDF membrane and incubated with the appropriate antibodies. The protein bands were visualized by enhanced chemiluminescence with the Super Signal detection kit (Thermo/Pierce, Rockford, IL, USA).

Immunofluorescence staining. The primary AECs or lung specimens were fixed in 4% paraformaldehyde, stained with the appropriate primary antibodies and incubated with FITC-conjugated anti-mouse IgG or Cy3-conjugated anti-rabbit IgG (Jackson ImmunoResearch, West Grove, PA, USA). The nuclei were stained with DAPI. Representative micrographs were observed using a confocal laser scanning microscope (TCS SP5; Leica, Wetzlar, Germany).

Cell viability and cell cycle analysis. NIH 3T3 cells were seeded in a 24-well plate and incubated with sorafenib in the presence or absence of TGF-β1 (5 ng/ml) for the indicated hours. After exposure to MTT for 3 h, the cells were lysed with the addition of 100 μl DMSO. Cell viabilities were measured at absorbances of 570 and 630 nm on a microplate spectrophotometer (Thermo MK3, Waltham, MA, USA).

For cell cycle analysis, NIH 3T3 cells were cultured in a 6-well plate and treated with TGF-β1 and/or sorafenib for 24 h. Thereafter, the cells were washed, fixed, stained with propidium iodide and analyzed for DNA content on a BD FACSCalibur flow cytometer (BD Biosciences).

EdU incorporation assay. After treatment with TGF-β1 and/or sorafenib for 48 h, NIH 3T3 fibroblasts were incubated with EdU (5-ethynyl-2′-deoxyuridine, 25 μM) in medium for an additional 3 h before fixation. Cell proliferation was assessed using the Cell-Light EdU Apollo488 *In Vitro* Imaging Kit (RIBOBIO, Guangzhou, China) according to the manufacturer's instructions. Samples were then observed under an Olympus IX51 microscope at $\times$20 magnification. The incorporation ratio of EdU-labeled cells was finally measured according to the abundance of Hoechst staining. At least 2000 cells were counted for each group using NIH ImageJ software.

Quantitative real-time PCR (real-time qPCR). Total RNA isolation and reverse transcription were performed essentially as previously described.[18] The real-time qPCR analysis was run on the MX3000p system (Stratagene, La Jolla, CA, USA) using SYBR Green PCR Master Mix (Toyobo, Tokyo, Japan). Each measurement was repeated in triplicate and normalized to the corresponding GAPDH content values. The primers optimized for real-time PCR assays are listed in Supplementary Table 1.

BLM-induced pulmonary fibrosis. Briefly, male mice weighing 23–25 g were allowed free access to food and water containing 350 mg/l dissolved phenobarbital for 1 week. At day 0, the mice maintained under chloral hydrate anesthesia (500 mg/kg) were intratracheally injected once only with 3.5 mg/kg BLM. The mice in the sham-operated group ($n=10$) were given saline only. At day 3 after intratracheal BLM injection, the BLM-treated mice were randomized into two groups that received vehicle or sorafenib until the end of the experiment. The sorafenib-treated group ($n=20$) received the drug by gavage once per day at a dose of 5 mg/kg body weight, which is approximately one-third of the human dose used in clinical therapy. The sham-operated and BLM groups ($n=20$) received an identical dose of normal saline. All of the animals were killed after 2 or 4 weeks, and lung biopsies were collected for the assays described below.

Histological and immunohistochemical analyses. The lung specimens were fixed in 4% paraformaldehyde, dehydrated in a graded alcohol series and embedded in paraffin blocks. Five-micron-thick sections were then stained with hematoxylin and eosin for routine examination or Sirius red for the visualization of collagen deposition. The lung sections were immunostained with antibodies against E-cadherin, α-SMA or FSP1 at a dilution of 1 : 500. The same concentration of normal mouse IgG served as a negative control. The bound antibodies were eventually visualized using 3,3′-diaminobenzidine as a chromogen (Dako), and the slides were counterstained with hematoxylin.

Hyp determination. As an indirect measure of tissue collagen content, the Hyp levels in the lung tissue (100 mg) were determined according to a modified method described by Jamall *et al*.[45] The Hyp content was expressed in micrograms of Hyp per gram of wet weight (μg/g). The number of Hyp measurements was the same as the number of animals in each group.

Statistical analysis. All of the assays were performed in triplicate. The data are presented as the mean values ± S.E. Comparisons were made using the Student's *t*-test or analysis of variance. A two-sided *P*-value <0.05 was considered statistically significant for all analyses.

Conflict of Interest

The authors declare no conflict of interest.

Acknowledgements. This work was supported by grants from the National Basic Research Program of China (2009CB941103 and 2011CBA01105) and the National Science and Technology Major Projects (2011ZX09307-302-01) to X. Ding; grants from the National Science Foundation of China (81170011), the Science and Technology Commission of Shanghai Municipality (11430702100, 114119b2200, 12DJ1400103, 124119a9000, 12411950105 and 12DZ1942500) and the International Science and Technology Cooperation Program of China (2011DFB30010) to H.P. Li; and grants from the National Basic Research Program of China (2013CB967103) and the National Natural Science Foundation of China (31000624 and 81272396) to Y.L. Chen.

Author contributions

Y.L.C., X.Z., H.P.L. and X.D. conceived the project, designed experiments and wrote and edited the manuscript. Y.L.C., X.Z., J.B., L.G., X.L.Y., L.Z. and Q.X. performed experiments. Y.X.Z. and L.X. conducted data analysis. All authors read, revised and approved the final manuscript.

1. Bjoraker JA, Ryu JH, Edwin MK, Myers JL, Tazelaar HD, Schroeder DR *et al.* Prognostic significance of histopathologic subsets in idiopathic pulmonary fibrosis. *Am J Respir Crit Care Med* 1998; **157**: 199–203.
2. King TE Jr, Pardo A, Selman M. Idiopathic pulmonary fibrosis. *Lancet* 2011; **378**: 1949–1961.
3. Raghu G, Weycker D, Edelsberg J, Bradford WZ, Oster G. Incidence and prevalence of idiopathic pulmonary fibrosis. *Am J Respir Crit Care Med* 2006; **174**: 810–816.
4. Raghu G, Collard HR, Egan JJ, Martinez FJ, Behr J, Brown KK *et al.* ATS/ERS/JRS/ALAT Committee on Idiopathic Pulmonary Fibrosis. An official ATS/ERS/JRS/ALAT statement: idiopathic pulmonary fibrosis: evidence-based guidelines for diagnosis and management. *Am J Respir Crit Care Med* 2011; **183**: 788–824.
5. Iwano M, Plieth D, Danoff TM, Xue C, Okada H, Neilson EG. Evidence that fibroblasts derive from epithelium during tissue fibrosis. *J Clin Invest* 2002; **110**: 341–350.
6. Willis BC, Liebler JM, Luby-Phelps K, Nicholson AG, Crandall ED, du Bois RM *et al.* Induction of epithelial-mesenchymal transition in alveolar epithelial cells by transforming growth factor-beta1: potential role in idiopathic pulmonary fibrosis. *Am J Pathol* 2005; **166**: 1321–1332.
7. Kim KK, Kugler MC, Wolters PJ, Robillard L, Galvez MG, Brumwell AN *et al.* Alveolar epithelial cell mesenchymal transition develops in vivo during pulmonary fibrosis and is regulated by the extracellular matrix. *Proc Natl Acad Sci USA* 2006; **103**: 13180–13185.
8. Selman M, Pardo A. Role of epithelial cells in idiopathic pulmonary fibrosis: from innocent targets to serial killers. *Proc Am Thorac Soc* 2006; **3**: 364–372.
9. Blobe GC, Schiemann WP, Lodish HF. Role of transforming growth factor beta in human disease. *N Engl J Med* 2000; **342**: 1350–1358.
10. Thiery JP, Acloque H, Huang RYJ, Nieto MA. Epithelial-mesenchymal transitions in development and disease. *Cell* 2009; **139**: 871–890.
11. Massagué J, Chen YG. Controlling TGF-beta signaling. *Genes Dev* 2000; **14**: 627–644.
12. Padua D, Massagué J. Roles of TGF-β in metastasis. *Cell Res* 2009; **19**: 89–102.
13. Miettinen PJ, Ebner R, Lopez AR, Derynck R. TGF-β induced transdifferentiation of mammary epithelial cells to mesenchymal cells: involvement of type I receptors. *J Cell Biol* 1994; **27**: 2021–2036.
14. Zavadil J, Bottinger EP. TGF-beta and epithelial-to-mesenchymal transitions. *Oncogene* 2005; **24**: 5764–5774.
15. Phan SH. Biology of fibroblasts and myofibroblasts. *Proc Am Thorac Soc* 2008; **5**: 334–337.
16. Khalil N, O'Connor RN, Unruh HW, Warren PW, Flanders KC, Kemp A *et al.* Increased production and immunohistochemical localization of transforming growth factor-beta in idiopathic pulmonary fibrosis. *Am J Respir Cell Mol Biol* 1991; **5**: 155–162.
17. Khalil N, Parekh TV, O'Connor R, Antman N, Kepron W, Yehaulaeshet T *et al.* Regulation of the effects of TGF-beta 1 by activation of latent TGF-beta 1 and differential expression of TGF-beta receptors (T beta R-I and T beta R-II) in idiopathic pulmonary fibrosis. *Thorax* 2001; **56**: 907–915.
18. Chen YL, Lv J, Ye XL, Sun MY, Xu Q, Liu CH *et al.* Sorafenib inhibits transforming growth factor β1-mediated epithelial-mesenchymal transition and apoptosis in mouse hepatocytes. *Hepatology* 2011; **53**: 1708–1718.
19. Escudier B, Eisen T, Stadler WM, Szczylik C, Oudard S, Siebels M *et al.* TARGET Study Group. Sorafenib in advanced clear-cell renal-cell carcinoma. *N Engl J Med* 2007; **356**: 125–134.
20. Llovet JM, Ricci S, Mazzaferro V, Hilgard P, Gane E, Blanc JF *et al.* SHARP Investigators Study Group. Sorafenib in advanced hepatocellular carcinoma. *N Engl J Med* 2008; **359**: 378–390.
21. Wilhelm SM, Carter C, Tang L, Wilkie D, McNabola A, Rong H *et al.* BAY 43-9006 exhibits broad spectrum oral antitumor activity and targets the RAF/MEK/ERK pathway and receptor tyrosine kinases involved in tumor progression and angiogenesis. *Cancer Res* 2004; **64**: 7099–7109.
22. Kasai H, Allen JT, Mason RM, Kamimura T, Zhang Z. TGF-β1 induces human alveolar epithelial to mesenchymal cell transition (EMT). *Respir Res* 2005; **6**: 56.
23. Cho HJ, Baek KE, Saika S, Jeong MJ, Yoo J. Snail is required for transforming growth factor-beta-induced epithelial-mesenchymal transition by activating PI3 kinase/Akt signal pathway. *Biochem Biophys Res Commun* 2007; **353**: 337–343.
24. Vancheri C, Failla M, Crimi N, Raghu G. Idiopathic pulmonary fibrosis: a disease with similarities and links to cancer biology. *Eur Respir J* 2010; **35**: 496–504.
25. Cheng S, Lovett DH, Gelatinase A. (MMP-2) is necessary and sufficient for renal tubular cell epithelial–mesenchymal transformation. *Am J Pathol* 2003; **162**: 1937–1949.
26. Nakao A, Fujii M, Matsumura R, Kumano K, Saito Y, Miyazono K *et al.* Transient gene transfer and expression of Smad7 prevents bleomycin-induced lung fibrosis in mice. *J Clin Invest* 1999; **104**: 5–11.
27. Chen YF, Feng JA, Li P, Xing D, Zhang Y, Serra R *et al.* Dominant negative mutation of the TGF-β receptor blocks hypoxia-induced pulmonary vascular remodeling. *J Appl Physiol* 2006; **100**: 564–571.
28. Abe K, Toba M, Alzoubi A, Koubsky K, Ito M, Ota H *et al.* Tyrosine kinase inhibitors are potent acute pulmonary vasodilators in rats. *Am J Respir Cell Mol Biol* 2011; **45**: 804–808.
29. Mejias M, Garcia-Pras E, Tiani C, Miquel R, Bosch J, Fernandez M. Beneficial effects of sorafenib on splanchnic, intrahepatic, and portocollateral circulations in portal hypertensive and cirrhotic rats. *Hepatology* 2009; **49**: 1245–1256.
30. Reiberger T, Angermayr B, Schwabl P, Rohr-Udilova N, Mitterhauser M, Gangl A *et al.* Sorafenib attenuates the portal hypertensive syndrome in partial portal vein ligated rats. *J Hepatol* 2009; **51**: 865–873.
31. Wang Y, Gao J, Zhang D, Zhang J, Ma J, Jiang H. New insights into the antifibrotic effects of sorafenib on hepatic stellate cells and liver fibrosis. *J Hepatol* 2010; **53**: 132–144.
32. Wu Z, Yang L, Cai L, Zhang M, Cheng X, Yang X *et al.* Detection of epithelial to mesenchymal transition in airways of a bleomycin induced pulmonary fibrosis model derived from an alpha-smooth muscle actin-Cre transgenic mouse. *Respir Res* 2007; **8**: 1–11.
33. Tanjore H, Xu XC, Polosukhin VV, Degryse AL, Li B, Han W *et al.* Contribution of epithelial-derived fibroblasts to bleomycin-induced lung fibrosis. *Am J Respir Crit Care Med* 2009; **180**: 657–665.
34. Yang J, Weinberg RA. Epithelial-mesenchymal transition: at the crossroads of development and tumor metastasis. *Dev Cell* 2008; **14**: 818–829.
35. Bechtel W, McGoohan S, Zeisberg EM, Müller GA, Kalbacher H, Salant DJ *et al.* Methylation determines fibroblast activation and fibrogenesis in the kidney. *Nat Med* 2010; **16**: 544–550.
36. Chang YS, Adnane J, Trail PA, Levy J, Henderson A, Xue D *et al.* Sorafenib (BAY 43-9006) inhibits tumor growth and vascularization and induces tumor apoptosis and hypoxia in RCC xenograft models. *Cancer Chemother Pharmacol* 2007; **59**: 561–574.
37. Sebolt-Leopold JS, English JM. Mechanisms of drug inhibition of signalling molecules. *Nature* 2006; **441**: 457–462.
38. Daniels CE, Wilkes MC, Edens M, Kottom TJ, Murphy SJ, Limper AH *et al.* Imatinib mesylate inhibits the profibrogenic activity of TGF-β and prevents bleomycin-mediated lung fibrosis. *J Clin Invest* 2004; **114**: 1308–1316.
39. Neef M, Ledermann M, Saegesser H, Schneider V, Reichen J. Low-dose oral rapamycin treatment reduces fibrogenesis, improves liver function, and prolongs survival in rats with established liver cirrhosis. *J Hepatol* 2006; **45**: 786–796.
40. Chaudhary NI, Roth GJ, Hilberg F, Müller-Quernheim J, Prasse A, Zissel G *et al.* Inhibition of PDGF, VEGF and FGF signalling attenuates fibrosis. *Eur Respir J* 2007; **29**: 976–985.
41. Tugues S, Fernandez-Varo G, Muñoz-Luque J, Ros J, Arroyo V, Rodés J *et al.* Antiangiogenic treatment with sunitinib ameliorates inflammatory infiltrate, fibrosis, and portal pressure in cirrhotic rats. *Hepatology* 2007; **46**: 1919–1926.
42. Daniels CE, Lasky JA, Limper AH, Mieras K, Gabor E, Schroeder DR. Imatinib-IPF Study Investigators. Imatinib treatment for idiopathic pulmonary fibrosis: Randomized placebo-controlled trial results. *Am J Respir Crit Care Med* 2010; **181**: 604–610.
43. Abraham V, Chou ML, DeBolt KM, Koval M. Phenotypic control of gap junctional communication by cultured alveolar epithelial cells. *Am J Physiol* 1999; **276**: L825–L834.
44. Chen YL, Liu B, Zhou ZN, Hu RY, Fei C, Xie ZH *et al.* Smad6 inhibits the transcriptional activity of Tbx6 by mediating its degradation. *J Biol Chem* 2009; **284**: 23481–23490.
45. Jamall IS, Finelli VN, Que Hee SS. A simple method to determine nanogram levels of 4-hydroyproline in biological tissues. *Anal Biochem* 1981; **112**: 70–75.

Supplementary Information accompanies this paper on Cell Death and Disease website (http://www.nature.com/cddis)